Theoretical Chemistry Accounts (2022) 141:30
https://doi.org/10.1007/s00214-022-02889-3

REGULAR ARTICLE

Rigid, strained, and flexible: a DFT study of a backbone-affected monohydride formation of salen and salan complexes

Mihály Purgel[1]

Received: 14 January 2022 / Accepted: 14 May 2022 / Published online: 30 May 2022

Abstract
The monohydride formation of some palladium(II)-sulfosalen and sulfosalan catalysts was studied by DFT methods. The coordination of the hydrogen molecule to the metal center and the following heterolytic dissociation of the coordinated hydrogen could occur in a two-step or a concerted process resulting in a monohydride complex and having a protonated dissociated phenolate arm. The effect of the backbone frame of the ligands (the molecular unit between two nitrogen atoms) strongly determines the energetics and the type of the hydride formation. Rigid, strained, and flexible molecular structures were studied covering a wide range of planar and spherical types of backbones. Besides the previously studied Direct 1 and Direct 2 mechanisms, three other mechanisms of direct monohydride formation were found. Known and fictive structures were studied to predict kinetically and thermodynamically preferred pathways as well as complexes for this type of reaction.

Keywords Density functional theory · Derivative · Diastereomer · Rotation · Water-soluble · Chelate ring

1 Introduction

Over the last decades, transition metal salen (N,N'-bis(salicylidene)ethylenediamine) complexes have been developed into effective catalysts. The main drawback, however, is their limited hydrolytic stability in aqueous media. To resolve this, salen can be hydrogenated to provide salan complexes. This also makes changes in catalytic activity, which is commonly attributed to the increased flexibility due to the saturation of the imine groups. The rigid Pd-salen and the hydrolytically stable and flexible Pd-salan complexes catalyze different types of catalytic processes: hydrogenation and/or redox isomerization [1–3], C–C coupling reactions [4–13].

In our previous paper [14], we have focused on the flexibility of the palladium(II)-sulfosalan complex (PdHSS) having an ethylene backbone between the two nitrogen atoms. The monohydride formation derived from molecular hydrogen in neutral (non-acidic) conditions was chosen as a reference reaction. We have studied the effect of the substitution by methylene groups on the phenolate arm (PdHSS-Me) and the nitrogen atom (PdHSS-NMe) and by chlorine, methyl, methoxy, and *tert*-butyl groups (PdHSS-PhCl, -PhMe, -PhOMe, -Ph*t*Bu) on the phenolic rings, as well. Both stereoisomers of the non-substituted salan complex (R,R and R,S) have also been investigated. Two main pathways have been studied: the direct (D) and the indirect hydride (ID) formation. The direct mechanism is a two-step process where the first step is a substitution of the hydrogen molecule and phenolate arm followed by a proton transfer from the coordinated hydrogen to the dissociated phenolate, while the ID is a three-step process including the substitution of the phenolate arm and a water (solvent) molecule, the substitution of hydrogen and water molecules and the final proton transfer. Depending on the direction of phenolate dissociation, i.e., the orientation of hydrogen molecule relative to the phenolate arm two types of D and ID can be defined. Figure 1 represents the orientation of the dissociating phenolate group and the coordinating hydrogen molecule of the D1 and D2 mechanisms. Since the D1 mechanism was found as the most favored among all studied mechanisms, in the present work, the direct mechanisms are discussed in detail. Due to the flexibility of the salan ligand, internal rotation of the phenolate arm of the saturated complex can also occur, which facilitates the monohydride formation in a concerned process skipping the intermediate of a coordinated hydrogen molecule. It had the lowest activation barrier among all

✉ Mihály Purgel
purgelmisi@gmail.com

[1] Department of Physical Chemistry, University of Debrecen, Egyetem tér 1, Debrecen 4032, Hungary

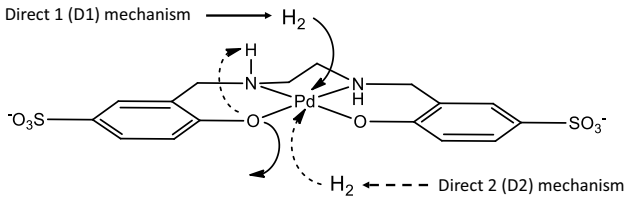

Fig. 1 Scheme of the Direct 1 and Direct 2 mechanisms representing the orientations of the dissociating phenolate arm and the coordinating hydrogen molecule

investigated mechanisms and set the D1 process definitely as the preferred one.

In our previous work [14] the hydride formation was also detected experimentally which was in good agreement with our computational results, since the monohydride formation has been found as an exergonic reaction by the DFT calculations. It occurred, however, only such a case when the stationary points, starting from the reference system as far as the final products, included the hydrogen molecule and two water molecules in addition to the metal complex. It means that at all points on the potential energy surface the small molecules (water and hydrogen) were weakly bound to each other as well as to the metal complex by a different type of hydrogen bond network. Note that if the stationary points were referred to as the energy of the separated PdHSS + H_2 + 2 H_2O molecules, the processes would have been strongly endergonic, excluding the detection of the hydride species. Due to the experimental results, the used theoretical model and methodology are adequate for further studies on similar systems. In the recent work, the effect of the different backbone types of the salan ligand is studied on the energetics. The main goal was to investigate the effects of the different structural units on the energetics and the mechanism as well. Palladium has been chosen to make a direct comparison to our previous computational study in which the "standard" ethylene backbone took place between the nitrogen atoms.

2 Methods

DFT calculations [15] were performed using the Gaussian09 software package [16]. Geometry optimizations were carried out with the M06 functional [17]. The Def2TZVP ECP/basis set was used for the palladium [18], together with the TZVP basis set for the non-metal atoms [19, 20]. Frequency calculations were made at the level of the theory of geometry optimization. The solvent (water) effect was accounted for by the Polarized Continuum Model (IEF-PCM) [21] as an implicit solvent model; however, explicit water molecules were also taken into account. Stationary points were confirmed by frequency analysis where minima had all positive frequencies and TSs had one imaginary frequency associated with the actual movement of the reaction coordinate. Relative free energies (ΔG) are reported at 298.15 K and atmospheric pressure. All stationary points were referred to a cluster including the given metal complex, the hydrogen molecule and two explicit water molecules. The orientation of the small molecules (hydrogen and water) was almost the same for all investigated derivatives to make a relevant comparison for them.

3 Results

The studied complexes are divided into two groups: i) "classical" salen and salan derivatives that can be easily derived from the basic forms and ii) derivatives having spherical backbones, see Fig. 2. In the i) group are Pd-sulfosalen (**1**), Pd-sulfosalan (**2**), along with 12 additional derivatives covering a wide range of rigid and flexible backbone forms: benzylidene (**3**)——called as salophan by Atwood [22]——, cyclohexylidene (**4**), bipyridyl (**5**), hydrogenated bipyridyl (**6**), dipyrrine (**7**) and its radical form (**8**)——idea of the species from a review by Thomas [23]——, methylidene (**9**), phenylmethylidene (**10**)——idea of the species from the article by Dewan [13]——, propylidene (**11**)——called as salpan by Atwood——, butylidene (**12**), pentylidene (**13**) and hexylidene (**14**) derivatives, while in the ii) group are ortho-carborane (**15**), dodecahedrane (**16**), twistane (**17**), pentamethylenetetramine (**18**)——derived from dinitrosopentamethylenetetramine and hexamethyltetraamine——, 1,4-diazacycloheptane (**19**), 1,3-diazacyclopentane (**20**)——idea of the species from the article by Roy et al. [24]——, and 1,3-diazacyclobutane (**21**) derivatives.

Due to the chiral nitrogen atoms, there are two diastereomers of the salan derivatives: in (R,R) the two hydrogens are oriented in the opposite direction, while in (R,S) they are oriented in the same direction. It is found that for each of the odd carbon chains (**9**, **10**, **11**, **13**) the (R,S) diastereomer is the more favorable by 3–4 kcal mol^{-1}. Surprisingly the (R,S) isomer of the benzylidene (**3**) and butylidene (**12**) derivatives is also slightly more favorable than the (R,R) isomer (ΔG = 0.5 and 0.9 kcal mol^{-1}). In the case of **3**, this can be explained by a less strain, while in the case of **12** it is because of the smaller repulsion between hydrogen atoms and the higher symmetry. **5**, **7,** and **8** have no hydrogen on the nitrogen, while in the case of **6** only the (R,R) orientation is possible sterically; the optimized structures of **5**, **6,** and **7** are represented in Fig. S1. Form **4** has many possible isomers and among them the (R,S) isomer is not unfavorable, although it is not a symmetrical form, see Fig. S2.

In the case of the hexylidene chain (**14**), another type of coordination mode is favorable, as the chain is long enough to form a NONO coordination mode instead of the

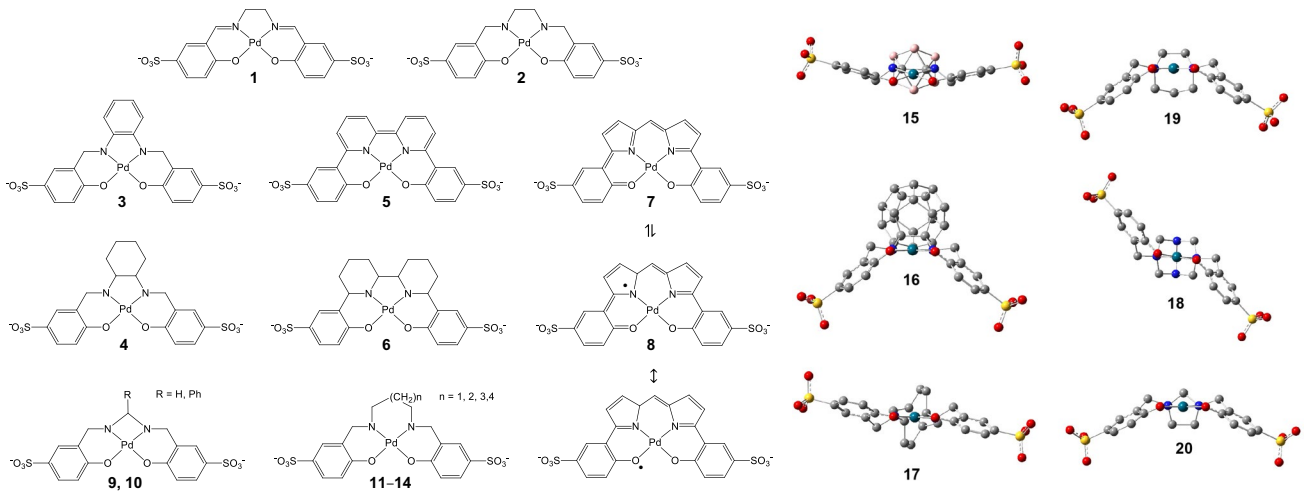

Fig. 2 Scheme of the salen and salan derivatives. **15**–**20** are optimized structures and the hydrogen atoms are omitted

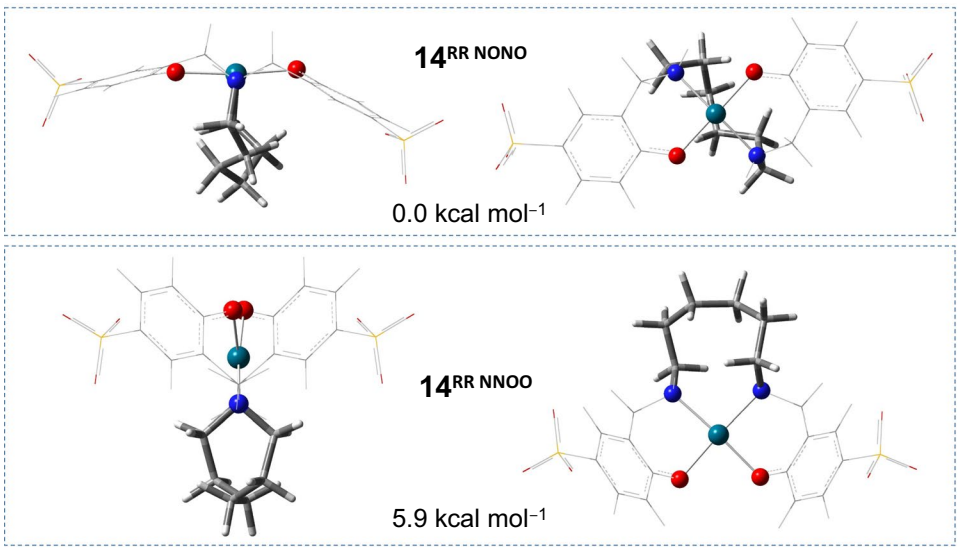

Fig. 3 The NONO and NNOO coordination modes of the optimized (R,R) isomers (assigned as ^{RR}) of the palladium hexylidene-salan derivatives

"classical" NNOO coordination mode, where the chain arches "above the NONO plane" forming a cage for the metal ion, see Fig. 3. In the case of (R,R) the NONO type is more favorable than NNOO by 5.9 kcal mol^{-1}, while the (R,S) forms are 12.7 and 6.8 kcal mol^{-1} higher in energy than the most favored species. In the case of the pentylidene (**13**) backbone, the NONO forms gave 7.9 (R, R) and 19.8 (S, R) kcal mol^{-1} higher forms energetically, while in the case of butylidene (**12**) the (R,R) it is by 17.5 kcal mol^{-1} higher.

In Fig. 4, the scheme of the previously discussed two Direct mechanisms (D1 and D2) can be seen together with the other three mechanisms of the Direct monohydride formation: Direct 3 (D3) belongs to the species **14,** while Direct 4 (D4) and Direct 5 (D5) belong to those species that will be discussed later. Note that in most cases the D2 mechanism resulted in a significantly higher barrier than D1, as in the case of the reference complex **2**. The **INT** and **P** forms are the intermediate and the product of the monohydride formation, respectively. In the case of **INT**, a coordinated hydrogen molecule is in the equatorial position, but in several cases, the phenolate–hydrogen substitution and the subsequent proton transfer of the D1 mechanism take place in a concerted process (**TS***) skipping the **INT** form, i.e., the monohydride was formed in one step. The D3 mechanism shows only concerted mechanisms, while D4 and D5 are two-step mechanisms.

The activation barriers of the monohydride formation of the D1 mechanism (both **TS1** and **TS2**) are in general higher in the case of the energetically favored (R,S) diastereomers.

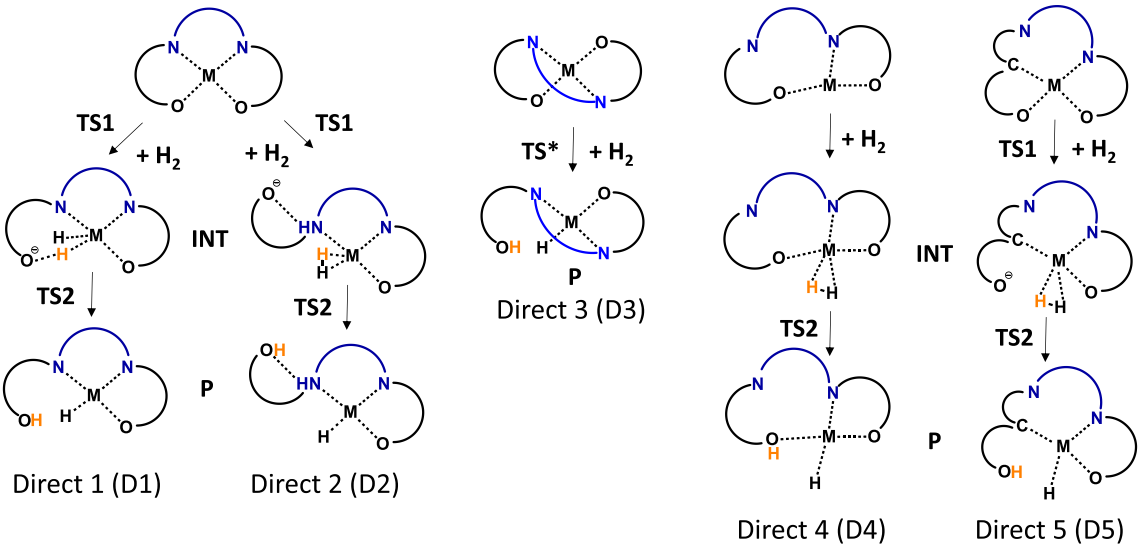

Fig. 4 Scheme of the Direct mechanisms discussed in this work. Transition states (TS), intermediates (INT), and products (P) are represented. TS* means a concerted process

It is worth mentioning that (R,S) and (R,R) cannot interconvert easily into each other due to the high activation barrier (discussed in the SI of Ref 14). Only the cadaverine-derived **13** shows a slightly lower barrier for the (R,S) isomer than for the (R,R) isomer. Since the (R,S) diastereomers are significantly more favored than the (R,R) isomers, it can be stated that mechanisms of (R,R) are inferior. In our previous study [14], we found that an internal phenolate arm rotation has a significant effect on the energetics since in most cases D1 mechanisms starting from the so-called half-stepped (assigned as hs) conformer result in a concerted process and having a lower activation barrier than the rate-determining step of the two-step processes. The half-stepped conformers of the (R,S) diastereomers, however, are in most cases energetically unfavored by ~ –5 kcal mol^{-1}, but the activation barrier of internal rotation is not significant, see our previous work. Half-stepped (arm rotated) conformers only in the case of **12** and **13** are relatively favored (1.5 and 0.6 kcal mol^{-1}).

In the case of **3** there are two competitive pathways due to the small energy difference of the diastereomers and the activation energies of the D1 mechanisms starting from them, see Table 1. It can be also seen that in the case of **4**, the D1 mechanism has lower activation energy than the D1 of the reference complex **2** which means the rigid cyclohexane backbone has a positive effect on the energetics. A very similar activation energy of D1 has been found in the case of **6,** but the D2 shows a lower barrier than in the case of **4** which means the "bilateral" rigidity brings the D1 and D2 mechanisms energetically closer together. The forms **9** and **10** show lower barriers than **2** due to the strain of the central four-chelate ring. In the case of **10**, the phenyl ring on methylidene significantly affects the barrier: **9** can be "expanded" with a phenyl ring which is more stable by 5.0 kcal mol^{-1} when the phenyl group is oriented to the same direction as the hydrogens of the amino groups than to the opposite direction. Almost identical barriers have been found for the species **11**–**13**; however, **11** and **12** show a concerted, while **13** shows a two-step mechanism. In the case of the NONO form of **14**, four possible phenolate dissociations are but only one is preferred due to the favorable hydrogen positions (23.6 vs. 28–31 kcal mol^{-1})——this direct pathway is declared as D3 due to the different coordination mode.

In the case of salen-type forms **5**, **7**, and **8** the activation barriers are similar to those of the reference complex **1**. The barriers of **7** and **8** are very similar which means the radical form does not show a significant difference in this type of process; only **TS2** of **8** was slightly more favorable than that of **7**. Salen derivatives have endergonic reactions, but the bipyridyl backbone is significantly more favored than the bipyrrine one: ΔG_r is 5.6 kcal mol^{-1} (**5**), 16.7 kcal mol^{-1} (**7**), and 13.0 kcal mol^{-1} (**8**), respectively. On the contrary, the products of the **3**, **4**, **6,** and **9**–**14** salan derivatives are energetically preferred, i.e., the reactions are exergonic (ΔG_r ~ –2–6 kcal mol^{-1}). It was also considered that the proton may even be transferred from the dissociated phenolate to one of the nitrogens, but these forms are ~ 10 kcal mol^{-1} higher in energy than **P**; therefore, their population is negligible.

Some (partially) fictive backbones have been also studied to describe the rigid and strained structural properties: (R,S) isomer of **15** and **16** is significantly more stable than (R,R) isomers; however, in the case of **17** the (R,R)

Table 1 The activation energies of the studied mechanisms of the palladium complexes. Data for **1** and **2** have been published in Ref. 14. (R,S) and (R,R) diastereomers assigned as ^{RR} and ^{RS}, the type of direct mechanism assigned as ^{D1}, ^{D2}, ^{D3}, ^{D4}, ^{D5}, the internal arm rotation, i.e., half-stepped conformer as ^{hs}, and the concerted process assigned as *

Complex number	TS1 ($\Delta^{\ddagger}G$)	TS2 ($\Delta^{\ddagger}G$)
1	24.3	24.3
2	18.1$^{RR\ hs\ D1*}$	19.1$^{RS\ D1*}$
(+1.7).^{RS}	23.1$^{RS\ D1*}$	
3	20.2.$^{RR\ D1}$	18.2.$^{RR\ D1}$
(− 0.5).^{RS}	27.5.$^{RR\ D2}$	24.5.$^{RR\ D2}$
	20.9$^{RS\ D1*}$	24.9.$^{RS\ D2}$
	25.4.$^{RS\ D2}$	
4	16.4$^{RR\ hs\ D1*}$	
(+3.0).^{RS}	23.0$^{RS\ hs\ D1*}$	
5	24.1	27.5
6	16.7.^{D1}	20.7.^{D1}
	20.2.^{D2}	21.3.^{D2}
7	27.1	32.0
8	27.3	31.1
9	16.8.$^{RR\ D1}$	16.5.$^{RR\ D1}$
(− 3.8).^{RS}	27.2.$^{RR\ D2}$	21.1.$^{RR\ D2}$
	17.8$^{RS\ hs\ D1*}$	17.0.$^{RS\ D1}$
	18.4.$^{RS\ D1}$	19.0.$^{RS\ D2}$
	24.6.$^{RS\ D2}$	
10	17.7.$^{RR\ D1}$	18.1.$^{RR\ D1}$
(− 5.0).^{RS}	**18.0.$^{RS\ D1}$**	**17.2.$^{RS\ D1}$**
	23.3.$^{RS\ D2}$	18.2.$^{RS\ D2}$
11	20.6.$^{RR\ D1}$	20.2.$^{RR\ D1}$
(− 3.3).^{RS}	27.4.$^{RR\ D2}$	27.1.$^{RR\ D2}$
	22.3$^{RS\ hs\ D1*}$	20.2.$^{RS\ D2}$
	22.3.$^{RS\ D2}$	
12	21.4$^{RR\ hs\ D1*}$	
	22.0$^{RS\ hs\ D1*}$	
13	22.9.$^{RR\ D1}$	22.3.$^{RR\ D1}$
(− 0.9).^{RS}	22.3.$^{RS\ D1}$	22.2.$^{RS\ D1}$
14	23.6^{D3*}	
15	21.7.$^{RR\ D1}$	23.5.$^{RR\ D1}$
(− 3.1).^{RS}	31.2.$^{RR\ D2}$	n.c
	26.6.$^{RS\ D1}$	n.c
	26.5.$^{RS\ D2}$	n.c
16	24.9$^{RS\ hs\ D1*}$	
17	22.1.$^{RR\ hs}$	21.8.$^{RR\ hs}$
(+1.6).^{RS}	25.0.^{RS}	24.4.^{RS}
18	22.3*	
19	20.8*	
20	13.1	8.1
21	15.9.^{D4}	

Bold values indicate the preferred pathway due to the lowest activation energy and/or the favored diastereomer

isomer is energetically favored, while other species have no diastereomers. In the case of **18** two conformers are very close in energy ($\Delta G = 0.8$ kcal mol^{-1}). **19** and **20**, however, have three conformers ($\Delta G = 1.1$ / 4.0 kcal mol^{-1} and 1.2 / 2.3 kcal mol^{-1}, respectively). All optimized isomers/conformers of **15**–**21** are represented in Fig. S3-S9. In the case of **20** and **21**, there are other relevant species, namely not only the well-known NNOO but also NCOO and NOO coordination modes are possible or even preferred where one of the nitrogen is dissociated from the palladium, see Fig. 5.

Regarding the monohydride formation, the D2 mechanism is slightly favored in the case of **15,** but the difference of the activation energies of D1 and D2 mechanisms is negligible (26.6 vs. 26.5 kcal mol^{-1}). This derivative is also interesting, while the arm-rotated (half-stepped) forms are less favored by 2–3 kcal mol^{-1} than the planar-type conformers. The monohydride formation of **15** is exergonic (-3.9 kcal mol^{-1}), while for **16**–**19** they are endergonic ($\otimes G_r$ ~ + 2–6 kcal mol^{-1}); however, forms **16**–**19** show lower activation barriers, see Table 1. In the case of the species having strained backbone (**9**, **10**), the H–O_{phen} distance and the H–Pd–O_{phen} angle are significantly shorter/smaller than in rigid complexes (**3**, **6**), while the shortest H–O_{phen} bond (196 pm) and H–Pd–O_{phen} angle (47°) occurs in the case of **18**, see the selected transition states in Fig. S10–S12.

The most interesting effects can be observed in the case of **20** and **21**. The species have the shortest N–N distances (214 and 196 pm) which are significantly shorter than that of the (R,S) isomer of **9** and **10** (233 pm). These differences cause, however, a huge effect on the energetics or the mechanism as well. Due to the large strain of the central chelate rings, the dissociation of the Pd–N bond of the saturated complex **20** shows significantly lower activation barriers than in the case of **9,** but in both cases, the **TS1** of hydrogen–phenolate substitution has lower energy than the TS of the Pd–N dissociation: 21.0 vs. 17.8 kcal mol^{-1} in **9** and 15.9 vs. 13.1 kcal mol^{-1} in **20**, respectively. In the case of **21,** the strain of the central chelate is so large that only the NOO coordination mode is relevant. The hydrogen molecule can coordinate to the vacant coordination site of the **21^{NOO}** species, and from them by a direct proton transfer to the phenolate arm results in the monohydride product, see Fig. 6—this direct pathway is declared as D4 due to the different coordination mode. Thermodynamically both **20** and **21** show strongly exergonic reaction: the relative energies of the monohydride products are -14.9 and -25.9 kcal mol^{-1}. Note that these species have quite different structures: NNOH and NOOH donor atoms are coordinated to the palladium which probably causes a significant difference in the hydrogenation processes. The monohydride formation starting from **21^{NCOO}** species has been also studied, but significantly higher activation barriers have been found, see Fig. S13——this direct pathway is declared as D5 due to the different coordination modes.

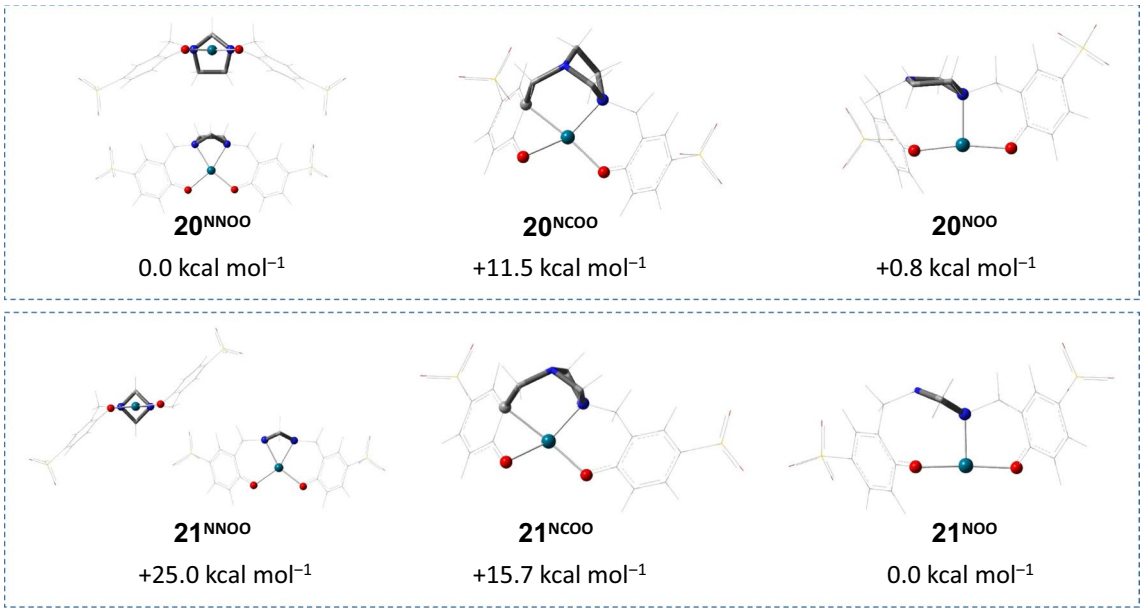

Fig. 5 Optimized structures of the isomers of the **20** and **21** species. ^{NNOO}, ^{NCOO}, and ^{NOO} assign the relevant diastereomers

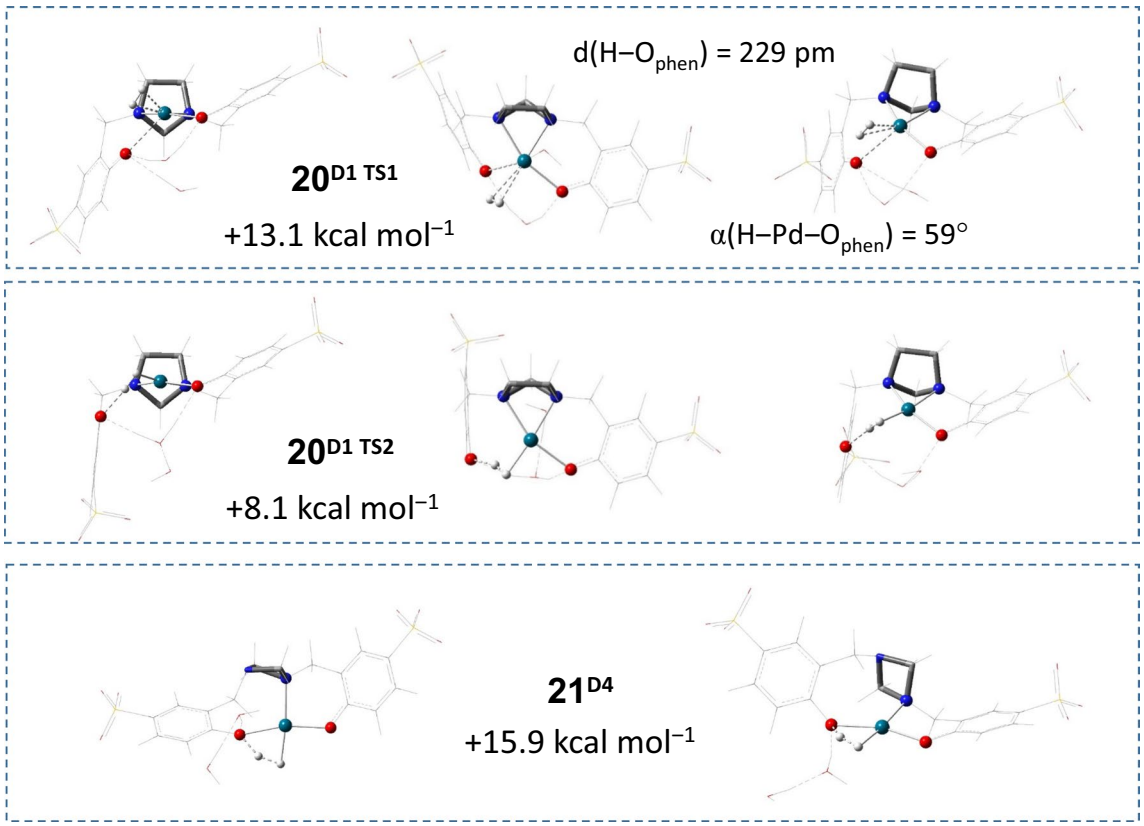

Fig. 6 Optimized structures of the **TS1** of the favored Direct mechanisms of the **20** and **21** palladium salan derivatives in different orientations

4 Conclusion

In this study, flexible, rigid, and strained types of backbones of salan and salen complexes have been studied to see how the different structural units affect the energetics and the mechanism of the monohydride formation from molecular hydrogen. In general, (R,S) diastereomer was found as the more stable isomer opposite to the reference complex which had (R,R) as a stable isomer. The increased rigidity (cyclohexylidene and hydrogenated bipyridyl backbones) showed lower activation barriers than the reference complex having ethylene backbone due to a large number of frozen degrees of freedom. Larger space-filled, spherical, or nearly spherical rigid symmetric backbones (ortho-carborane, dodecahedrane, etc.) may be advantageous primarily in terms of functionalization, as the dissociation of the phenolate arm is not more favored than the reference palladium-salan complex. The flexible backbones such as propylidene, butylidene, pentylidene, and hexylidene showed higher barriers than the reference one. The latter one, however, showed another type of coordination mode: instead of the well-known NNOO coordination mode, the NONO showed preference where the long hexylidene chain took place over the plane of the donor atoms. Complexes having strained backbones (methylidene and 1,3- diazacyclopentane) showed lower activation barriers than the reference one; however, the largest strain occurred by the 1,3- diazacyclobutane showed no preference for the NNOO coordination mode, but for the NOO one in which one of the palladium-nitrogen bonds was dissociated. The most exergonic reaction of the D1-type mechanism is belonging to the 1,3-diazacyclopentane backbone, while the "unusual" D4 mechanism of the 1,2-diazacyclobutane backbone predicts extremely favored monohydride products. In the latter case, there is a weakly bonded protonated phenolate arm, while in the case of the D1 mechanism the protonated phenolate arm is fully dissociated. Salen derivatives and most of the spherical backbone salan derivatives show endergonic reactions for the monohydride formation, while other salan derivatives including the ortho-carborane backbone are exergonic.

Supplementary Information The online version contains supplementary material available at https://doi.org/10.1007/s00214-022-02889-3.

Authors Contributions M.P. contributed to conceptualization; M.P. contributed to formal analysis; M.P. contributed to the investigation; M.P. contributed to methodology; M.P. provided the resources; M.P. contributed to writing—original draft preparation; M.P. contributed to writing—review and editing.

Funding Open access funding provided by University of Debrecen. This work was partially supported by the European Union and the European Social Fund through project Supercomputer, the National Virtual Lab, grant no.: TÁMOP-4.2.2.C-11/1/KONV-2012–0010.

Availability of data and material All data analyzed during this study are included in this published article and its supplementary information file.

Code availability Not applicable.

Declarations

Conflict of interest The authors have no conflicts of interest to declare that are relevant to the content of this article.

Competing interests Authors are required to disclose financial or non-financial interests that are directly or indirectly related to the work submitted for publication.

References

1. Ayala V, Corma A, Iglesias M, Rincón JA, Sánchez F (2004) Hybrid organic—inorganic catalysts: a cooperative effect between support, and palladium and nickel salen complexes on catalytic hydrogenation of imines. J Catal 224:170
2. Voronova K, Purgel M, Udvardy A, Bényei AC, Kathó Á, Joó F (2013) Hydrogenation and redox isomerization of allylic alcohols catalyzed by a new water-soluble Pd−tetrahydrosalen complex. Organometallics 32:4391–4401
3. Lihi N, Bunda S, Udvardy A, Joó F (2020) Coordination chemistry and catalytic applications of Pd(II)-, and Ni(II)-sulfosalan complexes in aqueous media. J Inorg Biochem 203:110945
4. Liu P, Feng XJ, He R (2010) Salen and half-salen palladium(II) complexes: synthesis, characterization and catalytic activity toward Suzuki-Miyaura reaction. Tetrahedron 66:631–636
5. Yuan L, Xu Y, Hu X, Yang G, Wu Y (2015) A water-soluble palladium-salen catalyst modified by pyridinium saltshowing higher reactivity and recoverability for Heck couplingreaction. J Mol Cat A: Chemical 396:55–60
6. Pessoa JC, Correia I (2019) Salan vs. salen metal complexes in catalysis and medicinal applications: Virtues and pitfalls. Coord Chem Rev 388:227–247
7. Liu YS, Gu NN, Liu P, Ma XW, Liu Y, Xie JW, Dai B (2015) Water-soluble salen-Pd complex as an efficient catalyst for Suzuki-Miyaura reaction of sterically hindered substrates in pure water. Tetrahedron 71:7985–7989
8. Heo Y, Kang YY, Palani T, Lee J, Lee S (2012) Inorg Chem Comm 23:1–5
9. Bunda S, May NV, Bonczidai-Kelemen D, Udvardy A, Vincent Ching HY, Nys K, Samanipour M, Van Doorslaer S, Joó F, Lihi N (2021) Copper(II) complexes of sulfonated salan ligands:

thermodynamic and spectroscopic features and applications for catalysis of the Henry reaction. Inorg Chem 60(15):11259–11272
10. Bunda S, Voronova K, Kathó A, Udvardy A, Joo F (2020) Palladium (II)–Salan complexes as catalysts for Suzuki–Miyaura C–C Cross-coupling in water and Air. Effect of the various bridging units within the diamine moieties on the catalytic performance. Molecules 25:3993–4013
11. Voronova K, Homolya L, Udvardy A, Bényei AC, Joó F (2014) Pd–tetrahydrosalan-type complexes as catalysts for sonogashira couplings in water: efficient greening of the procedure. ChemSusChem 7:2230–2239
12. Bunda S, Udvardy A, Voronova K, Joo F (2018) Organic solvent-free, Pd(II)-salan complex-catalyzed synthesis of biaryls via suzuki-miyaura cross-coupling in water and air. J Org Chem 83:15486–15492
13. Dewan AA (2014) A highly efficient and inexpensive palladium-salen complex for room temperature Suzuki-Miyaura reaction. Bull Korean Chem Soc 35:1855–1858
14. Purgel M, Feher PP, Balogh AK, Bunda S, Joo F (2021) Water-mediated formation of hydride derivates from flexible Pd-salan complexes: a DFT study. Mol Cat 500:111311
15. Parr RG, Yang W (1989) Density Functional theory of atoms and molecules. Oxford University Press, New York
16. Frisch MJ, Trucks GW, Schlegel HB, Scuseria GE, Robb MA, Cheeseman JR, Scalmani G, Barone V, Mennucci B, Petersson GA, Nakatsuji H, Li X, Caricato M, Li X, Hratchian HP, Izmaylov AF, Bloino J, Zheng G, Sonnenberg JL, Hada M, Ehara M, Toyota K, Fukuda R, Hasegawa J, Ishida M, Nakajima T, Honda Y, Kitao O, Nakai H, Vreven T, Montgomery JA, Jr., Peralta JE, Ogliaro F, Bearpark MJ, Heyd JJ, Brothers EN, Kudin KN, Staroverov VN, Kobayashi R, Normand J, Raghavachari K, Rendell AP, Burant JC, Iyengar SS, Tomasi J, Cossi M, Rega N, Millam JM, Klene M, Knox JE, Cross JB, Bakken V, Aadamo C, Jaramillo J, Gomperts R, Stratmann RE, Yazyev O, Austin AJ, Camni R, Pomelli C, Ochterski JW, Martin RL, Morokuma K, Zakrewski VG, Voth GA, Salvador P, Dannenberg JJ, Dapprich S, Daniels AD, Farkas Ö, Foresman JB, Ortiz JV, Cioslowski J, Fox DJ (2009) Gaussian 09, Revision E.01, Gaussian, Inc., Wallingford
17. Zhao Y, Truhlar DG (2008) The M06 suite of density functionals for main group thermochemistry, thermochemical kinetics, noncovalent interactions, excited states, and transition elements: two new functionals and systematic testing of four M06-class functionals and 12 other functionals. Theor Chem Acc 120:215–241
18. Andrae D, Haeussermann U, Dolg M, Stoll H, Preuss H (1990) Energy-adjusted ab initio pseudopotentials for the second and third row transition elements. Theor Chim Acta 77:123–141
19. Schaefer A, Horn H (1992) Fully optimized contracted Gaussian-basis sets for atoms Li to Kr. J Chem Phys 97:2571–2577
20. Schaefer A, Huber C, Ahlrichs R (1994) Fully optimized contracted Gaussian-basis sets of triple zeta valence quality for atoms Li to Kr. J Chem Phys 100:5829–5835
21. Miertuš S, Scrocco E, Tomasi J (1981) Electrostatic interaction of a solute with a continuum. A direct utilization of ab initio molecular potentials for the prevision of solvent effects. Chem Phys 55:117–129
22. Atwood DA (1997) Salan complexes of the group 12, 13 and 14 elements. Coord Chem Rev 165:267–296
23. Thomas F (2016) Ligand-centred oxidative chemistry in sterically hindered salen complexes: an interesting case with nickel. Dalton Trans 45:10866–10877
24. Roy S, Lima S, Ribeiro N, Correia I, Avecilla F, Kuznetsov ML, Pessoa JC, Kaminsky W, Dinda R (2021) Synthesis, characterization and DFT studies of novel –CH2– capped and non-capped salan complexes. Inorg Chim Acta 519:120265–120272